

## Influence of exterior infill walls on the performance of RC frames under tsunami loads: Case study of school buildings in Sri Lanka

Marta Del Zoppo<sup>a,\*</sup>, Kushan Wijesundara<sup>b</sup>, Tiziana Rossetto<sup>c</sup>, Priyan Dias<sup>d</sup>, Marco Baiguera<sup>c</sup>, Marco Di Ludovico<sup>a</sup>, Julian Thamboo<sup>e</sup>, Andrea Prota<sup>a</sup>

<sup>a</sup> Department of Structures for Engineering and Architecture, University of Naples Federico II, Italy

<sup>b</sup> Department of Civil Engineering, University of Peradeniya, Sri Lanka

<sup>c</sup> EpiCentre, University College London, United Kingdom

<sup>d</sup> Department of Civil Engineering, University of Moratuwa, Sri Lanka

<sup>e</sup> Department of Civil Engineering, South Eastern University, Sri Lanka

### ARTICLE INFO

#### Keywords:

VDPO-BI  
Tsunami assessment  
School resilience  
Breakaway masonry infill walls  
RC frames  
Froude number

### ABSTRACT

This paper assesses the structural performance of RC frame buildings subjected to tsunami-induced loads, accounting for the influence of exterior masonry infill walls on the overall structural performance. Both the in-plane and out-of-plane contributions of masonry infill walls are considered in the analysis. To illustrate the importance of accounting for exterior infill walls in the response of structures to tsunami, two case study buildings are considered and modelled in 3D. The first case study is a typical two-storey school building in Sri Lanka, and the second is a modified version of this design configuration proposed in Sri Lanka after the 2004 Indian Ocean Tsunami to provide more redundancy against scour. Through these case studies, the effect of the non-uniform distribution of infill walls in the building and their failure (or “breakaway”) on building performance is considered. The building performance is characterized by a number of response parameters (i.e., first yielding, development of two hinges, and shear failure in ground floor columns). The paper shows that the in-plane behaviour of exterior infill walls increases the flexural capacity and lateral stiffness of the structure, as would be expected. However, it also shows that an assumption of non-breakaway infill walls consistently leads to premature structural failure mechanisms, associated with the concentration of drag forces on seaward columns only. The results demonstrate that a good estimation of the location and occurrence of shear failure in structural elements can only be achieved by explicitly considering the out-of-plane behaviour and failure of exterior infill walls during an incremental tsunami load analysis. Finally, the Froude number assumed for the analysis is seen to strongly affect the performance of both structural and non-structural components, highlighting the importance of choosing realistic tsunami properties to perform a reliable capacity assessment.

### 1. Introduction

Developing reliable performance assessment approaches for structures in tsunami hazard zones has recently gained significant attention. Indeed, reducing post-disaster downtime of critical facilities and improving the resilience of coastal communities are challenging tasks. Education facilities play a crucial role in community resilience after natural disasters, bringing societal life back to normalcy [1]. There is, therefore, a need to realistically estimate the structural performance of existing buildings under tsunami induced loads, accounting for all features that can influence their structural behaviour. In this context, this

paper contributes towards understanding the role of exterior infill walls on the structural performance of buildings during a tsunami inundation. This allows for a reliable damage assessment (and relevant downtime) of existing reinforced concrete (RC) frame buildings with masonry infill walls subjected to tsunami induced loads.

When a tsunami inundates a coastline, the tsunami flow imparts drag (i.e., hydrodynamic) pressure and uplift forces on buildings. Drag pressure acts on the building envelope, and the pressure magnitude is a function of the exposed surface in the plane normal to the tsunami flow direction [2]. In the context of infilled RC frame structures, exterior infill walls attract a large portion of the drag pressure acting on the building.

\* Corresponding author.

E-mail address: [marta.delzoppo@unina.it](mailto:marta.delzoppo@unina.it) (M. Del Zoppo).

<https://doi.org/10.1016/j.engstruct.2021.111920>

Received 4 July 2020; Received in revised form 13 January 2021; Accepted 18 January 2021

Available online 13 February 2021

0141-0296/© 2021 Elsevier Ltd. All rights reserved.

If effectively connected, the infill walls can transfer these forces to the surrounding RC frame, resulting in high lateral loads on seaward structural elements, such as columns. Conversely, in the case of a weak connection between masonry infill walls and surrounding frame, or in the case of large openings, the lateral loads transferred to seaward columns are low as the infill walls are more likely to fail i.e., out of their plane. When the infill walls fail out of their plane, often termed break-away infill walls, the tsunami lateral load applied to seaward members suddenly reduces. However, as water enters the building, drag forces are applied to interior vertical members as well, and uplift forces are exerted on elevated slabs of the flooded structure [3,4]. Hence, exterior infill walls may significantly contribute to the overall performance of frame structures during a tsunami. Furthermore, the action of infill walls oriented in a parallel direction to the tsunami flow also plays an important role in the overall lateral-load resisting mechanism [6].

A literature review on available performance assessment approaches for structures under tsunami loading shows that exterior infill walls in the plane normal to the flow direction are usually assumed fully connected to the surrounding frame; thus, out of plane failure is not attained during tsunami inundation (i.e., termed non-breakaway infill walls) [7–12]. Only few existing studies consider the in-plane contribution of infill walls to lateral resistance under tsunami loads [6,13,14]. Nanayakkara and Dias [15] account for both out-of-plane and in-plane failure of infill walls as separate cases for deriving structural collapse fragility curves via Monte Carlo simulations.

However, only the studies of Del Zoppo et al. [3,4] explicitly consider the progressive out-of-plane failure of infill walls during the tsunami inundation. These studies demonstrate that the progressive out-of-plane failure of infill walls significantly influences both drag and uplift forces acting on structures during a tsunami inundation, resulting in changes to the local and global structural performance. The present paper extends these studies by considering the role of infill walls in the tsunami structural assessment of an existing RC structure with a non-uniform infill walls distribution. A typical two-storey school building in Sri Lanka is herein adopted as a case study. Indeed, Sri Lanka experienced significant damage and losses during the 2004 Indian Ocean Tsunami, since most of its physical development takes place near the coastline. Furthermore, school safety represents a crucial aspect for the disaster risk reduction policy in Sri Lankan local communities [16]. Sri Lankan school buildings typically present a standard type plan, with only minor variations in foundation and infill details. Thus, any insights generated from the study of a typical school building has the potential of reducing the risk for a very large number of school buildings and its users. The typical school building is a slender RC frame, designed for gravity loads only, with exterior masonry infill walls asymmetrically distributed along the building perimeter (i.e., in-plan asymmetry). Therefore, the configuration and orientation of masonry infill walls may have significant impacts on overall or local structural performance during a tsunami. This study analyses typical Sri Lankan school buildings in the original configuration and in an improved configuration that includes design modifications suggested by the Sri Lankan Society of Structural Engineers (SSE) after the 2004 Indian Ocean Tsunami [17]. The study consists of numerical analyses on 3D FEM models of the case-study buildings, performing the Variable Depth Pushover analysis for Breakaway Infilled frames (VDPO-BI) [3,4]. The VDPO-BI explicitly considers the effects of the presence and failure of exterior infill walls on the size and distribution of horizontal and vertical loads (i.e., drag forces and uplift) during the analysis. The analyses assume a single direction for the tsunami flow, coincident with one of the two principal directions of the case-study buildings. Under this assumption, infill walls in the plane normal to the tsunami flow work only out of their planes. Conversely, infill walls in the plane parallel to the tsunami flow work only in their plane. The combined in-plane and out-of-plane behaviour of masonry infill walls is out of the scope of the present work and will be investigated in future studies where multi-directional tsunami flows are considered.

To fully understand the influence of infill walls in the response of structures to tsunami, several models are herein analysed: (i) bare frame with exterior infill walls broken away in both directions (this serves as a reference to point out the structural capacity neglecting the contribution of infill walls); (ii) frame with exterior infill walls still standing in-plane but damaged out-of-plane (this captures the contribution of infill walls working in their plane); (iii) frame with exterior infill walls undamaged both in-plane and out-of-plane (this shows the effect of masonry infill walls working out of their plane on the overall structural performance). Interior masonry walls (e.g., partitions) are neglected in the analyses. The achievement of selected performance levels is investigated and compared for all configurations. A sensitivity analysis on structural and non-structural component capacities with respect to the tsunami flow velocity, expressed by means of the Froude number, is also presented.

The novelty of this research paper consists in performing the VDPO-BI structural analysis methodology developed by the authors [4] on 3D case-study buildings to illustrate the role of exterior masonry infill walls (considering both their in-plane and out-of-plane contributions) on the local and global structural performance and damage progression. The results clearly demonstrate the importance of considering both the in-plane contribution of infill walls (especially when asymmetrical), and their progressive out-of-plane failure during the tsunami performance assessment of existing RC buildings with masonry infill walls. The choice of a typical Sri Lankan school building as a case-study will ensure great practical benefit. Indeed, outcomes from this research are applicable to a large number of existing structures that house a vulnerable segment of the population. Final considerations on the effectiveness of design modifications suggested by the SSE are derived based on the analysis results, and alternatives for improving the performance of school buildings under tsunami inundation are proposed.

## 2. Methodology

The loading imparted by a tsunami inundation on buildings is complex due to the combination of unsteady and quasi-steady flow regimes that characterise the different stages of the incoming and outgoing tsunami flow around buildings. However, Foster et al. [18] and McGovern et al. [19] have shown that due to the extremely large wavelengths of tsunamis, the tsunami inundation is prolonged and sustained, leading to large hydrodynamic forces acting on the structure. The corresponding flow regime can be considered quasi-steady since the temporal variation of the flow is small, especially with respect to the length scale of a building.

Tsunami on-shore flows induce a complex combination of loads on buildings, comprising horizontal and vertical forces [20,21]. These forces are to be resisted by the structural system and its foundations, the capacity of which may be reduced due to buoyancy and scouring effects [22]. The methodology herein adopted only assesses the capacity of structural systems under tsunami induced horizontal (i.e., hydrodynamic or drag) and vertical (i.e., uplift) loads, computed as discussed in the following sections. Other tsunami-induced loads or phenomena, such as bore, scour or debris impact, have not been included in the analysis methodology due to their impulsive or highly uncertain nature.

### 2.1. Structural analysis

The performance of structural systems under tsunami loading is assessed through a refined non-linear static analysis methodology where the Variable Depth Pushover approach (VDPO, introduced by Petrone et al. [7] and later modified in Baiguera et al. [23]), is adapted to be able to simulate the effects of infill wall failure on the loading protocol. This approach summarised here and is termed Variable Depth Pushover for Breakaway Infilled frames (VDPO-BI) [3,4]. The VDPO-BI allows for a realistic assessment of the structural performance during a tsunami inundation, accounting for the actual distribution and capacity of infills in the outer perimeter of a building. Indeed, an asymmetrical plan

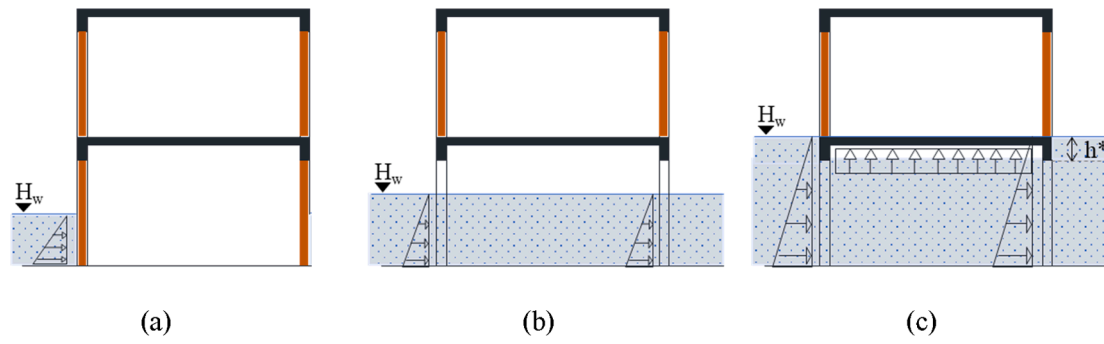


Fig. 1. Tsunami-induced loads for increasing tsunami inundation depth,  $H_w$ : (a) before the collapse of ground storey masonry infill walls, (b) after the collapse of ground storey masonry infill walls and (c) when the water depth reaches the soffit of the first storey beams, inducing internal buoyancy.

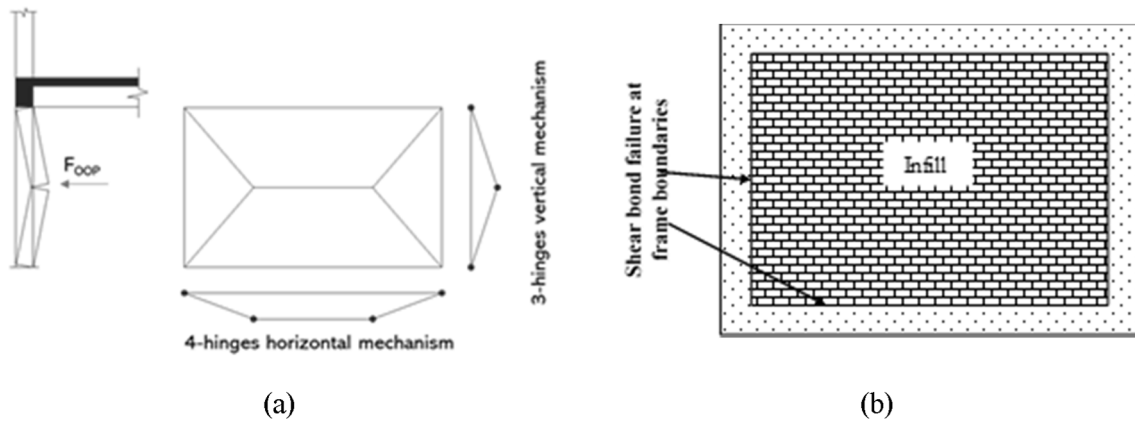


Fig. 2. Out-of-plane failure mechanism of infill walls: (a) flexural and (b) shear failure.

distribution of exterior infill walls can lead to an eccentric performance of the building that cannot be captured if the role of such walls is neglected.

In the VDPO-BI, the tsunami inundation depth ( $H_w$ ) at the site of the structure is monotonically increased (assuming a constant Froude number, as in the VDPO [7]). The corresponding horizontal forces are imparted to the building until the out-of-plane capacity of exterior infill walls (appropriately accounting for openings if any) in the plane normal to the tsunami flow direction is achieved. Up until this point, the water is assumed to act solely on the exterior of the building, and hence only the seaward columns are directly loaded by tsunami-induced drag forces, see Fig. 1a. Once the exterior infill walls fail, it is assumed that the water can pass through the building, inducing drag forces on interior columns, in proportion to their impacted surfaces. The new lateral loads on the interior and exterior members are calculated at the inundation depth at which the infill walls have failed, see Fig. 1b. Within this analysis model, partitions are not considered to contribute to the structural capacity. Typically, interior partitions are weaker than external infill walls, and hence they are herein assumed to be washed away when the inundation depth causes the failure of exterior infill walls [4]. From this point, the inundation depth is again monotonically increased, and corresponding forces applied to the interior and exterior structural components. When the inundation depth reaches the soffit of the first storey beams, vertical loads due to internal buoyancy (i.e., uplift loads) also begin to be applied to the slabs and beams, as required by ASCE 7-16 (Fig. 1c). This procedure is repeated for each storey of the building during the non-linear incremental analysis until the maximum lateral capacity of the structure is reached.

In the VDPO-BI, drag and uplift forces are applied to columns and beams respectively, in the form of load time-histories determined as a function of the increasing inundation depth. This allows the

modification of the load magnitude and distribution on members as a function of the failure of exterior infill walls during the incremental analysis. The exterior infill walls oriented in the plane normal to the tsunami flow are susceptible to out-of-plane (i.e., OOP) failures, related to the development of flexural or shear sliding mechanisms depending on the geometrical and mechanical properties of the infill walls (Fig. 2).

In the absence of experimental tests on masonry infill walls subjected to a triangular load distribution simulating the pressure induced by a tsunami flooding, the OOP flexural failure mechanism of masonry walls is addressed through the development of a double arch mechanism with a 3-hinge arch in the vertical direction and a 4-hinge arch in the horizontal direction, as described in Del Zoppo et al. [4] and shown in Fig. 2a. The OOP flexural capacity of the infill,  $F_{OOP}$ , can be computed as follows:

$$F_{OOP}(x) = 6N_v(t - c_v)\frac{w}{h} - 6N_v\left(\frac{w}{h} - 1\right)x - 3N_v x + 6N_h(t - c_h) - 3N_h x \quad (1)$$

In this equation,  $x$  is the OOP displacement at the centre of the panel;  $N_v$  and  $N_h$  are the resultants of compressive stresses in the vertical and horizontal arch, respectively;  $c_v$  and  $c_h$  are the compressed zone depths in vertical and horizontal arch, respectively;  $t$  is the panel thickness;  $w$  and  $h$  are width and height of the infill, respectively. The formulation is able to account for the different boundary conditions of the masonry infills at the surrounding frame. The presence of openings (i.e., windows or doors) is not accounted for in Eq. (1), which refers to full masonry infill walls only. Openings would reduce the value of  $F_{OOP}$ , which would need to be estimated by say numerical modelling. They do not figure in the case study that follows in Section 3, since doors and windows are located only on longitudinal front walls that are not framed by columns; such walls, and also longitudinal half walls at the rear of the building, are taken as having negligible OOP capacity.

Conversely, the OOP shear capacity depends on the interface shear

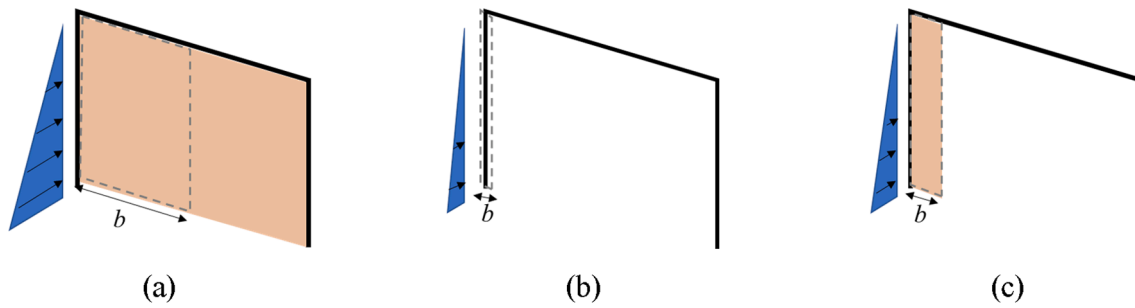


Fig. 3. Impacting surface for the calculation of drag forces on columns: (a) infill walls still standing, (b) infill walls totally broken away and (c) infill walls/partitions broken away with remaining parts of masonry attached to the surrounding frame.

bonding between masonry infill and surrounding frame, Fig. 2b. The OOP shear strength of masonry walls is a function on the mechanical properties of the thin layer of mortar at the infills boundaries and can be computed in accordance with Eurocode 6 [24]. However, to achieve such a failure mode the masonry wall should have a monolithic behaviour under the tsunami loading.

Therefore, the OOP flexural/shear capacity of exterior infill walls should be computed case by case to account for the different possible failure scenarios under tsunami inundation, and the thresholds for the definition of load time-histories on structural members established, as further discussed in Section 4.2.2.

## 2.2. Drag forces

Recent investigations by Qi et al. [25] and Foster et al. [18] have led to an experimentally validated set of equations for predicting the tsunami drag forces on buildings,  $F_D$ . The drag force formulation varies depending on the flow regime at the building, which is described by the Froude number of the impacting flow (i.e.,  $Fr = u/\sqrt{gH_w}$ , with  $u$  the flow velocity,  $g$  the gravitational acceleration and  $H_w$  the inundation depth). When  $Fr$  is less than a critical value,  $Fr_c$ , the flow regime is subcritical and the inundation depth at the front and back of the building is similar; for  $Fr > Fr_c$ , the flow condition is choked, there is a significant lowering of the inundation depth at the back of the building with respect to the front, and a hydraulic jump forms downstream. According to Foster et al. [18], the net drag force acting on a rectangular obstacle of width  $b$  subjected to a steady flow is:

$$F_D = 0.5C_D\rho u^2 H_w \text{ if } Fr < Fr_c \quad (2)$$

$$F_D = \lambda_s g^{1/3} u^{4/3} H_w^{4/3} \text{ if } Fr \geq Fr_c$$

where  $\rho$  is the sea water density (1.2 t/m<sup>3</sup> in order to account for suspended sediment),  $C_D$  is the drag coefficient, and  $\lambda_s$  is the leading coefficient for steady flows, computed as a function of the blocking ratio,  $B/w$ , as follows:

$$\lambda_s = 0.73 + 1.2(B/w) + 1.1(B/w)^2 \quad (3)$$

Small blocking ratios are representative of a sparse urban environment (e.g.,  $B/w = 0.1$ ), while large values may reflect the conditions of a dense urban area (e.g.,  $B/w = 0.6$ ) [18].

The net drag force is then converted into a triangular horizontal pressure distribution acting on the building [7]. The definition of the drag pressures on structural members is strictly related to the failure of infill walls, that induces a modification in the intensity of drag forces (due to the reduction of  $b$ ) and in their distribution on structural members (i.e., exterior only or both exterior and interior). The failure of the infill walls is reached when the drag force acting on the wall (i.e., with  $b$  equal to the wall length) exceeds the OOP flexural/shear capacity of the infill wall.

Hence, the width  $b$  for computing the drag force on each column may not be constant during the VDPO-BI, and depends on the damage

condition of the masonry walls oriented in the plane normal to the tsunami flow direction (i.e., whether still standing or broken away) [4]. The definition of  $b$  is of paramount importance for the definition of drag load histories on vertical structural members to perform the VDPO-BI analysis. If the exterior infill wall is still standing (i.e., undamaged),  $b$  is equal to the infill length for central columns and half infill length for corner columns (Fig. 3a) and the drag forces are applied only to seaward structural members (Fig. 1a). Conversely, if the exterior infill walls are broken away during the analysis,  $b$  can be assumed to be equal either to the column width (Fig. 3b), or to the column width plus a tributary part of masonry (exterior walls or partitions) that remains attached to the surrounding frame (Fig. 3c). This choice depends on the connection between masonry walls and surrounding frame and represents a source of uncertainty during the performance assessment of infilled RC frames. Both assumptions are herein considered during the structural analysis after the failure of exterior infill walls, based on the infill wall and partition distribution and their connection to exterior/interior columns. Given the uncertainty related to the quantity of masonry remaining attached to the frame, an average tributary width of 0.5 m is tentatively assumed herein to account for this effect.

## 2.3. Uplift forces

Uplift forces are generally caused by a combination of hydrostatic and hydrodynamic components of the tsunami flow. The overall hydrostatic uplift caused by buoyancy can result in a complete failure of the building due to a global overturning mechanism [26]. This is likely to occur only when the building is relatively impermeable to the flow (i.e., non-breakaway infill walls) and high uplift forces develop at the foundation level. In the case of buildings with breakaway infill walls, the uplift pressure due to buoyancy is negligible compared to the lateral load components, and hence the effect on buoyancy on foundations is not herein considered.

As indicated in the ASCE 7-16 design provisions [2], hydrostatic uplift forces can also be produced on elevated floor levels by internal buoyancy due to the effect of trapped air below slabs (i.e., air pockets between slab and beams), submerged slabs and enclosed space where exterior walls do not break away.

The uplift pressure caused by the air pockets and submerged slabs can be computed as follows:

$$p = \rho g h^* \quad (4)$$

where  $h^*$  is the height of the beams including the slab thickness (Fig. 1c).

The buoyancy due to enclosed spaces may also produce significant uplift pressure on elevated slabs, depending on the out-of-plane capacity of exterior infill walls. However, if the infill walls are non-uniformly distributed over the perimeter frames, no enclosed spaces will form. Hence this load component is not considered herein, but more details on the effects of uplift loads due to enclosed space on structures can be found in [3,27] and will be object of future investigation.

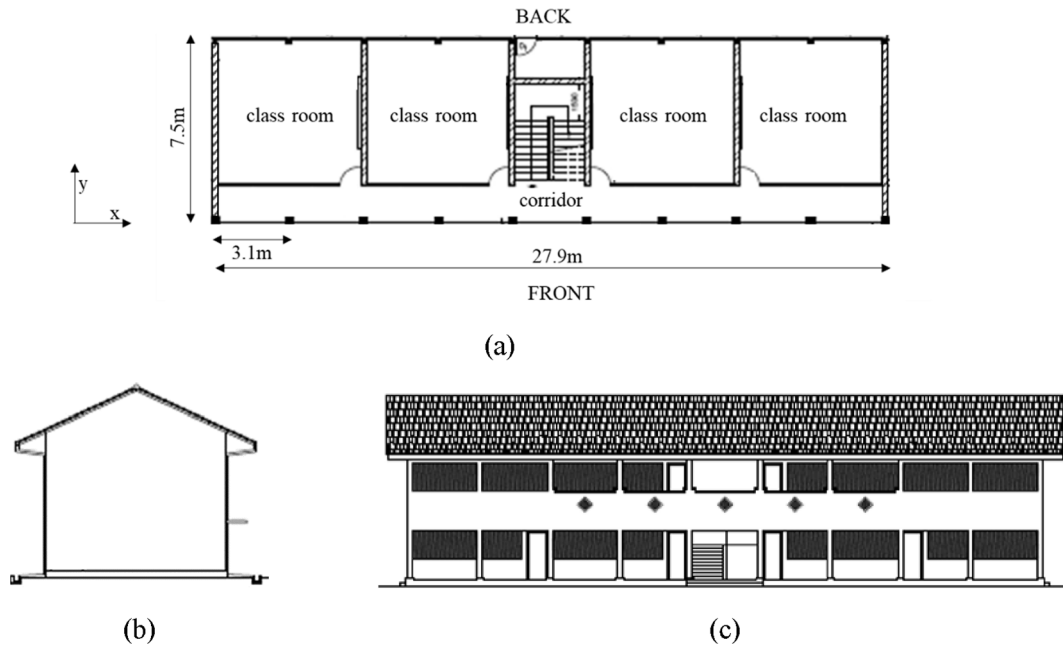


Fig. 4. Typical two-storey school building configuration: (a) ground floor type plan, (b) elevation in longitudinal direction – view from front, (c) elevation in transverse direction.

Although hydrodynamic tsunami-induced vertical loads include impulsive pressures caused by surge uplift [14,21], these are highly transient in nature and are neglected in the VDPO-BI analysis.

### 3. Case study

A two-storey school building in Sri Lanka has been chosen as a case-study to assess the influence of exterior infill walls on the performance of RC frame structures under tsunami loadings. Two configurations have been selected for this study. The first, termed typical school design, has a configuration and detailing that is widely used in coastal provinces of Sri Lanka well before the 2004 tsunami. In fact, as most schools are built by the government and follow a standard design and layout, this case-study is representative of many schools in Sri Lanka. The second school configuration is similar in layout and design as the typical school but contains design improvements that were proposed by the Sri Lankan Society of Structural Engineers (SSE) for increasing tsunami resilience against scour failure after the 2004 Indian Ocean Tsunami, and referred to as SSE design.

#### 3.1. Typical school design

The typical Sri Lankan school building is a two-storey RC frame structure with solid clay brick masonry infill walls, as shown in Fig. 4. The floor plans of the building are regular, with floor dimensions of 27.9

m and 7.5 m in length and width, respectively. Each floor plan comprises 4 classrooms besides the stair void and a storeroom. The building has a 7.5 m wide single bay in the y direction and 9 bays of 3.1 m width in x direction (Fig. 4a). The storey height is 3.0 m.

Full solid burnt clay brick masonry walls with 225 mm thickness serve as exterior infill walls in the transverse y direction (Fig. 4b). The plan distribution of the exterior infill walls in the x direction is not uniform, since an open corridor to access the classrooms is provided on the front longitudinal frame of both floors (Fig. 4c). Conversely, half infill walls (i.e., 900 mm height) with 115 mm thickness are placed below the windows of the rear frame. This geometrical asymmetry of non-structural components plays an important role when assessing the performance of the structure under lateral loading.

Reinforcement details of all beam and column cross-sections are illustrated in Fig. 5. The columns have a 225 mm × 225 mm cross-section with longitudinal reinforcement consisting of 4 φ16 bars, and transverse reinforcement of φ6 stirrups spaced at 150 mm. The concrete cover thickness is 25 mm. Beams have a 225 mm × 550 mm cross-section in the y direction, according to the strong beam-weak column hierarchy typical of structures designed for gravity loads only, without considering the capacity-based design concept for lateral loads. These beams support the one-way spanning RC slab in the x direction, of typical thickness 115 mm. Beams in the x direction have a 225 mm × 225 mm cross-section.

The foundation system of the typical school design consists of RC pad

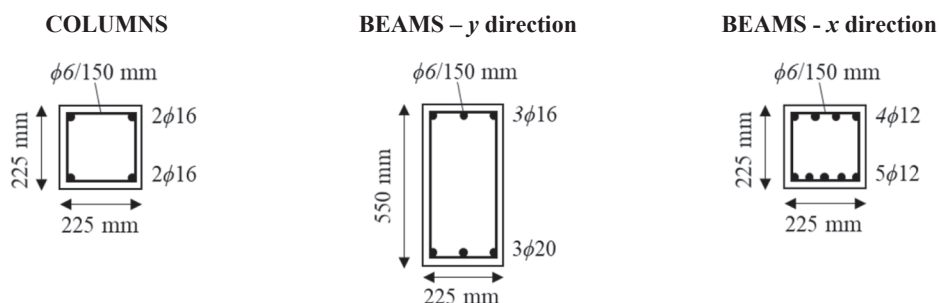


Fig. 5. Typical cross-sections of columns and beams for the 2-storey school building.



Fig. 6. Damage after the 2004 tsunami on existing schools caused by the scour.

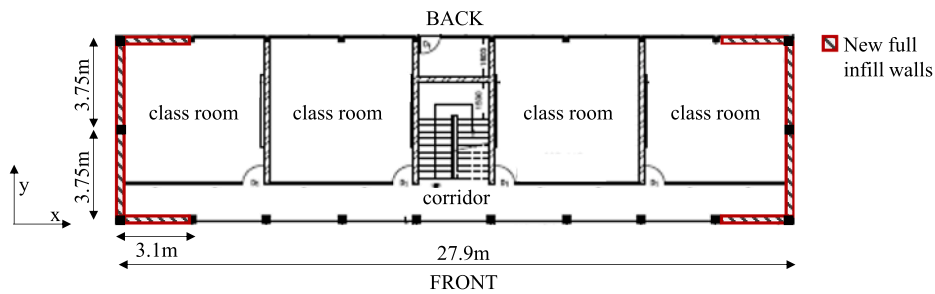


Fig. 7. Type plan of the SSE school design.

footings connected by masonry brickwork, as visible in Fig. 6b.

### 3.2. SSE design

Post-disaster surveys carried out after the 2004 tsunami indicated that partial collapse of some school buildings occurred because of the scour of sandy soil, causing the corner column foundations to lose their support. This failure mechanism was mainly related to the absence of a proper foundation system in the typical design school building. If both corner footings were affected by scour, collapse of the end bays was observed [28,29], as shown in Fig. 6a. However, in other cases it was also observed that this partial collapse was avoided due to the redundancy provided by the exterior infill walls still standing, as shown in Fig. 6b.

These observations led to the Sri Lankan Society of Structural Engineers issuing a set of guidelines for improved design of schools [17]. The guidelines include the provision of: (i) an additional central column in the end frames in the  $y$  direction of the building; (ii) RC plinth beams at ground level for the whole building; and (iii) full infill walls in the end bays (for both  $x$  and  $y$  directions) that would not fail or break-away during the tsunami inundation. These measures, depicted in Fig. 7, are intended to provide additional redundancy to the school against scour [28].

The SSE design does not modify the typical dimensions and details of structural members. Hence, the same cross-sections for columns and beams are used as in the typical design configuration (Fig. 5). According to the SSE design, the additional new columns have same cross-section of other columns. The new non-breakaway infill walls can be of varied materials with greater out-of-plane strength than solid clay brickwork. Hence it could be assumed that the exterior infill walls are non-breakaway, whatever the construction technology adopted.

However, in recognition that non-breakaway infill walls can be hard to achieve in practice, in this paper the case where the new infill walls do break away is also considered, in order to assess the change in structural

performance resulting from the additional structural members only.

## 4. Finite element model

### 4.1. Structural model

The two case-study school building configurations are modelled as 3D frames, and the VDPO-BI is performed in the OpenSees software [30]. The RC frames are modelled using force-based nonlinear beam-column elements [31,32] assuming five Gauss-Lobatto integration points. Each integration point represents a fibre section to monitor section forces and deformations. Geometric nonlinearities, such as P-Delta effects, are considered in the finite element model. Beam-column joints are modelled by joining concurrent nodes, and no rigid links are adopted.

For this study, the shear failure of members is evaluated on the analysis results employing the capacity model suggested by the Eurocode 8 Part 3 [33], in order to account for the effective axial load acting on structural members at each step of the analysis.

Details of the cross-section of beams and columns adopted for the typical and SSE design school configurations are presented in Fig. 5. The material properties adopted in the finite element model are discussed in Section 4.3.

A rigid diaphragm is adopted for simulating the effect of the first storey slab. Conversely, no constraint is used for the top of the first storey columns, due to the absence of the slab at the roof level. Base nodes are fixed to the ground.

### 4.2. Infill walls model

Several models are currently available in literature for considering the combined in-plane and out-of-plane capacity of masonry infill walls in the seismic assessment of RC frames [34,35, among many others]. However, the use of such refined models for the tsunami performance



**Fig. 8.** Out of plane failure modes observed in infill walls of school buildings in Sri Lanka under the 2004 Tsunami: (a) tsunami mainly acting along the  $x$  direction, and (b) tsunami mainly acting along the  $y$  direction.

assessment of RC buildings would not be significantly beneficial under the assumption of unidirectional flows. Indeed, under unidirectional tsunami flow, the in-plane capacity of infill walls is not affected by the damage experienced out of their plane. Conversely, the out-of-plane capacity and failure of infill walls affect the magnitude and distribution of tsunami loads on structural members (Fig. 3). Hence, the OOP capacity of exterior infill walls should be assessed before the definition of load time-histories to perform the VDPO-BI analysis. Thus, the OOP behaviour of walls is not modelled in OpenSees, but is herein simulated independently through the analytical models discussed in Section 2.1, and then accounted for in the FEM model during the definition of the loading histories, as previously discussed in Section 2.2.

#### 4.2.1. In-plane behaviour of exterior infill walls

Full and half exterior masonry walls are modelled as equivalent diagonal struts to represent their stiffness and strength contributions to the in-plane behaviour of RC frames [36]. Equivalent diagonal struts are widely accepted for modelling masonry panels in infilled RC frames under seismic action as a simple and rational modelling technique [37]. Internal partitions are not considered in the model, due to the presence of openings (i.e., doors or corridor) that inhibit the activation of the strut.

The corotational truss element available in the OpenSees software is adopted for modelling the in-plane behaviour of exterior masonry infill walls. The width of compressive struts is estimated using the equivalent strut model proposed by FEMA 365 [38]. For the case study, widths of the struts are approximately 1200 mm and 600 mm respectively, for the full and half masonry walls. The same strut properties are adopted for the SSE school configuration, assuming that only the OOP failure is prevented, while the in-plane capacity of the non-breakaway masonry infill walls would not change significantly.

#### 4.2.2. Out-of-plane behaviour of exterior infill walls

Fig. 8a and b show the OOP failures experienced by infill walls in the  $y$  and  $x$  directions, respectively, of typical school buildings in Sri Lanka during the 2004 tsunami inundation. Post-tsunami survey observations showed that the full infill walls in the  $y$  direction developed an OOP flexural failure (Fig. 8a) consistent with the double arch mechanism (Fig. 2a). Hence, this predominant failure mode is considered herein for evaluating the OOP capacity of these walls. A 4-edge boundary condition is considered, based on the good connection between infill walls and upper beams visible in Fig. 8a. The maximum OOP flexural capacity,  $F_{OOP}$ , of the full walls according to Eq. (1), is equal to 160 kN.

Conversely, half walls were fully washed away under the tsunami (Fig. 8b), as a result of the OOP shear failure. However, given the

reduced thickness of the half walls and the low shear bond resistance of infill to concrete frame [39] for the case study building, the half walls are assumed to break away at the beginning of the VDPO-BI.

#### 4.3. Material properties

The non-linear mechanical behaviour of concrete in compression is modelled with the *Concrete04* material, representing the uniaxial Popovics material [40] with degraded linear unloading/reloading stiffness according to the work of Jirsa and Karsan [41]. Given the minimal transverse reinforcement and low axial load in columns, the confinement effect of the core concrete is neglected. Grade 20 concrete is typically used in the construction of the two-storey type plan school buildings in Sri Lanka. Hence, a mean concrete compressive strength of 20 MPa is adopted in the model. The strain at the peak strength of the concrete is taken as 0.002, which is a commonly accepted assumption for unconfined concrete.

A bilinear stress-strain envelope, *Steel02* in OpenSees [42], is adopted for the steel reinforcement. The yield strength, modulus of elasticity and the strain-hardening ratio for steel material used as internal reinforcement in the school buildings are 460 MPa, 200 GPa and 0.5%, respectively.

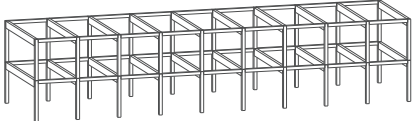
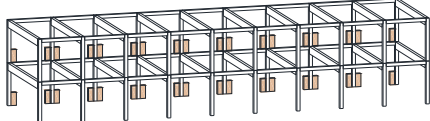
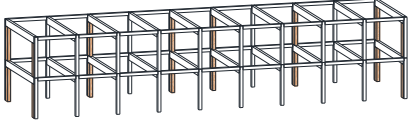
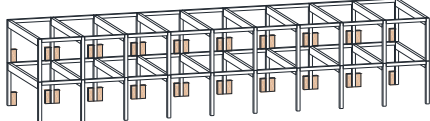
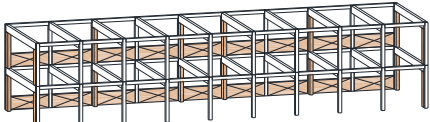
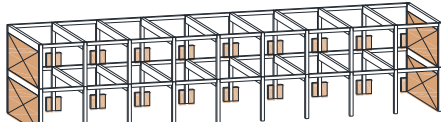
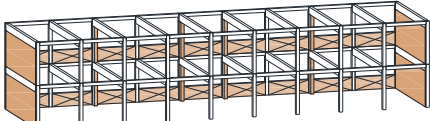
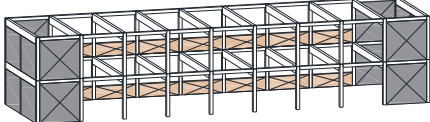
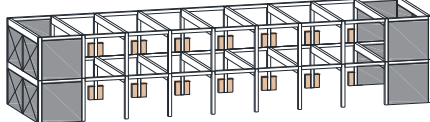
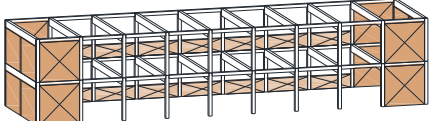
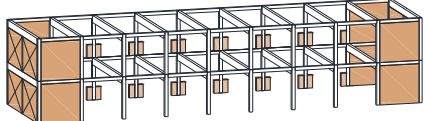
The in-plane behaviour of masonry infill struts is characterized by the stress-strain curve of the masonry under compression. The analytical model proposed by Hemant et al. [43] is used to define the compressive stress-strain curve for the masonry. In this model, the stress-strain curve in the ascending branch is parabolic, and it is extended in the descending branch up to the corresponding point of 0.9 times the peak strength ( $0.9 f_m$ ). Beyond this point, the compressive stress drops linearly up to the residual compressive stress of  $0.2 f_m$  at a strain of twice the peak strain. Hence, the non-linear behaviour of the infill struts is well represented by the constitutive material *Concrete01* in OpenSees. The mechanical parameters for the Sri Lankan local masonry are taken from the study by Konthesingha et al. [44]. The peak compressive stress of the masonry is assumed as 1.4 MPa, corresponding to a peak strain of 0.0018, and the ultimate strain as 0.003.

#### 4.4. Loading

Gravity loads are uniformly applied on the  $y$  direction beams. Dead loads ( $D$ ) are considered equal to  $4.0 \text{ kN/m}^2$ . Additional line loads are applied to the beams where exterior infill walls and interior partitions are placed:  $14 \text{ kN/m}$  for exterior full walls and  $7 \text{ kN/m}$  for half walls and partitions.

Tsunami-induced loads ( $F_{TSU}$ ) are considered together with other

**Table 1**  
Investigated model configurations for tsunami oriented in x and y direction of the building.

Tsunami orientation	
<b>x direction</b>	<b>y direction</b>
T_X1 Bare frame configuration (infill walls totally washed away)	T_Y1 Bare frame configuration (infill walls totally washed away)
	
T_X2 Bare frame with infill walls partially washed away (load irregularity)	T_Y2 Bare frame with half-walls below the windows partially washed away (load irregularity)
	
T_X3 Frame with infill walls partially washed away (load irregularity) and half-walls working in-plane (geometric irregularity)	T_Y3 Bare frame with infill full walls working in-plane and half-walls below the windows partially washed away
	
T_X4 Infilled frame with progressive OOP failure of full walls and half-walls working in-plane (geometric irregularity)	-
	
SSE_X1 SSE design configuration with non-breakaway infill walls at end bays	SSE_Y1 SSE design configuration with non-breakaway infill walls at end bays
	
SSE_X2 SSE design configuration with breakaway infill wall at end bays	SSE_Y2 SSE design configuration with breakaway infill walls at end bays
	

loads acting on the structure. This study adopts the load combination  $0.9D + F_{TSU}$  indicated by the ASCE 7-16 [2]. No live loads are accounted for, assuming a full evacuation of the school building occurs before the tsunami inundation.

The drag pressure is calculated adopting a blocking ratio  $B/w = 0.1$ , given the sparse urban environment typical of Sri Lankan coastal communities, with a resulting leading coefficient  $\lambda_s = 0.861$ . The drag pressure on columns is discretized into 5 forces per storey, applied as time-histories assuming a constant load application location during the VDPO-BI.

Uplift loads due to internal buoyancy are applied to the y direction beams as uniformly distributed time-histories during the incremental analysis. For the case study building, the maximum uplift pressure is  $p = 6.5 \text{ kN/m}^2$ . Uplift forces are applied to beams as uniform load time-histories with magnitude computed for each step of the increasing inundation depth. Drag and uplift forces are applied simultaneously to the structure during the VDPO-BI analysis, as shown in Fig. 1. However, uplift forces assume a non-null value only when the inundation depth reaches the soffit of the beams, generating internal buoyancy.

## 5. Results and discussion

### 5.1. Investigated infill model configurations

To assess the influence of in-plane and out-of-plane behaviour of exterior masonry infill walls on the overall structural behaviour, several configurations with increasing levels of model complexity are investigated. Several detailed initial assumptions are made (see also the Introduction) to account for the damage experienced by the masonry infill walls during the tsunami (i.e., bare frame with infill walls broken away, frame with infill walls still standing in-plane but collapsed out-of-plane, frame with infill walls still standing both in-plane and out-of-plane), as summarized in Table 1. The VDPO-BI is conducted assuming the tsunami acting in a single direction that coincides with the x direction (X) or the y direction (Y) of the school building, respectively. The modelling strategy adopted in this work is based on the consideration that partitions have lower OOP capacity (due to reduced thickness and different boundary conditions) than exterior infill walls; and hence, if exterior infill walls fail under a certain inundation depth then it is assumed that partitions would also fail under the same load [45].

For the typical school building, four infill model configurations are analysed. Configuration 1 (i.e., T\_X1 and T\_Y1) consists of the bare frame, assuming that the infill walls are completely broken away in both



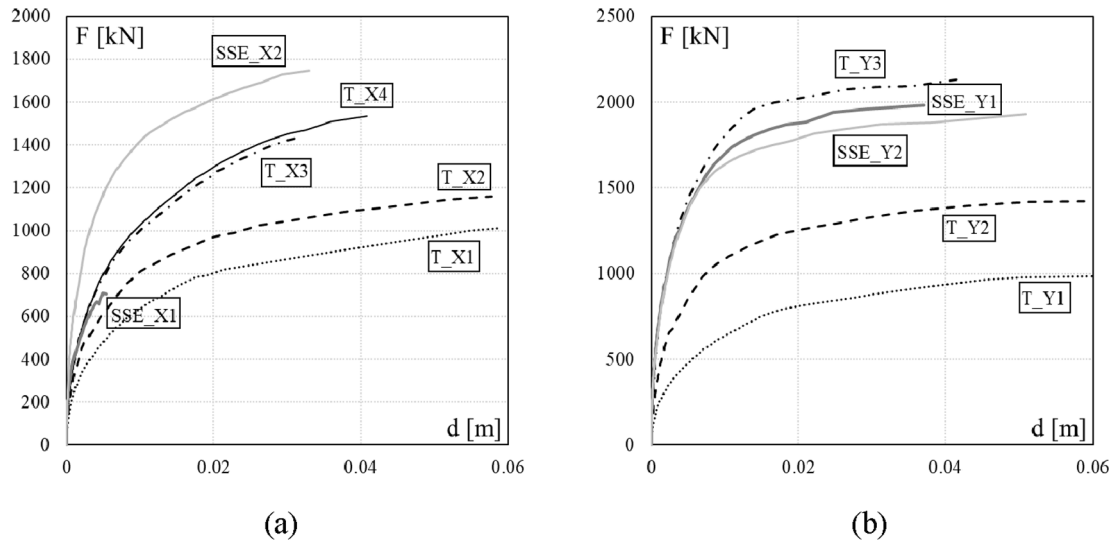


Fig. 9. Capacity curves for tsunami oriented in x direction (a) and y direction (b),  $Fr = 1$ .

directions. In configuration 2 (i.e., T\_X2 and T\_Y2), it is assumed that the infill walls are broken away, but a part of the masonry wall remains attached to the surrounding RC frame, as observed from post-tsunami surveys (Fig. 8). Given the asymmetrical plan distribution of interior and exterior walls, the portions of masonry still attached to the frame induce an eccentricity in the applied horizontal loads.

In configuration 3 (i.e., T\_X3 and T\_Y3), the in-plane capacity of the exterior infill walls parallel to the tsunami direction is accounted for and included in the model described in configuration 2. For configurations X1 to X3, it is assumed that the interior partitions are totally (T\_X1) or partially (T\_X2 and T\_X3) washed away by the tsunami flow, and hence their contribution to the gravity loads is neglected or reduced, respectively.

Configuration 4 applies only for a tsunami oriented in the x direction (i.e., T\_X4) and considers explicitly the out-of-plane failure of the exterior masonry walls as a function of the increasing inundation depth. Hence, the progressive failure of exterior walls is reflected in the definition of drag and uplift loads at each step of the VDPO-BI.

For the SSE design school building, two model configurations are analysed. A first configuration (i.e., SSE\_X1 and SSE\_Y1) considers that the infill walls of the specified exterior bays do not break away during the tsunami inundation. This model reflects the assumptions made in the SSE guidelines. A second configuration (i.e., SSE\_X2 and SSE\_Y2) takes into account only the design modification to the structure itself (additional columns) but adopts the breakaway masonry walls of the typical school building design. This is to point out the effectiveness of the structural improvements only, on the lateral capacity of the building

against tsunami loads.

5.2. Structural assessment under constant Froude number

The structural performance of the school buildings is first assessed performing the VDPO-BI with a constant Froude number (i.e.,  $Fr = 1$ ) for all the configurations shown in Table 1. This is done to investigate the effect of the in-plane and out-of-plane behaviour of masonry infill walls on the overall structural performance of the buildings.

The capacity curves obtained from the analysis up to a point of numerical instability are reported in Fig. 9 for tsunamis in x and y directions, in terms of base shear ( $F$ ) and top displacement ( $d$ ). The more realistic configurations for existing Sri Lankan school buildings are T\_X4 and T\_Y3; they display the highest flexural capacities in their respective directions for the typical structure. This might explain why such school buildings did not experience any global flexural failure during the 2004 tsunami. The SSE design configuration with non-breakaway infill walls, SSE\_X1 and SSE\_Y1, shows an overall poor performance compared to the typical school building configuration in the x direction. However, if traditional breakaway infill walls are adopted instead of non-breakaway ones, a lateral capacity and stiffness improvement can be achieved for tsunami in this direction (SSE\_X2) compared to the typical configuration (T\_X4), especially due to the new full walls in the x direction working in-plane. Conversely, in y direction, the configurations SSE\_Y1 and SSE\_Y2 experience a quite similar behaviour, and the typical configuration T\_Y3 shows a slightly better performance.

It should be noted that, when comparing the capacity curves, a

Table 2 Summary of results.

Configuration	F1			F2			S		
	$H_w$	$F$	IDR	$H_w$	$F$	IDR	$H_w$	$F$	IDR
	[m]	[kN]	[%]	[m]	[kN]	[%]	[m]	[kN]	[%]
T_X1	4.1	766	0.5%	4.6	968	1.5%	4.4	879	1.0%
T_X2	3.0	774	0.3%	3.6	1,125	1.4%	2.6	571	0.1%
T_X3	3.2	903	0.2%	4.1	1,440	1.1%	2.8	674	0.1%
T_X4	3.3	941	0.3%	4.1	1,456	1.0%	1.2	114	0.0%
SSE_X1	2.6	381	0.0%	3.4	651	0.1%	1.2	80	0.0%
SSE_X2	3.1	983	0.1%	4.0	1,667	0.8%	1.2	107	0.0%
T_Y1	4.2	755	0.5%	4.7	963	1.5%	4.5	877	1.0%
T_Y2	3.2	1,019	0.2%	3.8	1,371	1.2%	2.1	512	0.0%
T_Y3	3.8	1,365	0.1%	4.8	2,138	1.4%	2.0	484	0.0%
SSE_Y1	2.7	1,095	0.1%	3.3	1,598	0.2%	1.9	578	0.0%
SSE_Y2	3.6	1,443	0.2%	4.1	1,839	0.8%	2.1	571	0.0%

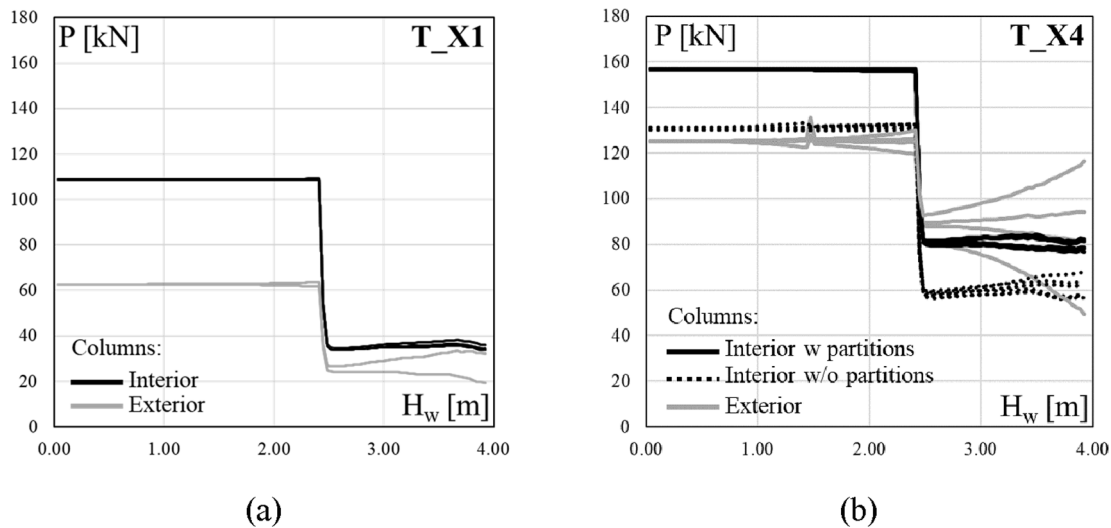


Fig. 10. Axial load in ground storey columns for configurations T\_X1 (a) and T\_X4 (b).

higher base shear may not correspond to a higher tsunami inundation depth. The base shear depends in fact on the overall drag force induced by the tsunami for a certain inundation depth, that is different for each configuration based on the impacting surface considered for each column.

To further assess the performance of different model configurations and the damage progression during the tsunami inundation, two performance levels have been defined herein for the flexural behaviour. One performance level (termed F1) consists in the achievement of first yield in longitudinal reinforcement of ground storey columns. A second performance level (termed F2) is defined as the first development of two hinges in a column, as it is considered the beginning of a flexural failure mechanism for the structure. An additional performance level (termed S) is considered for brittle mechanisms as the achievement of the first shear failure in ground storey columns. The main results at each defined performance level are summarized in Table 2, expressed in terms of inundation depth  $H_w$ , base shear,  $F$ , and interstorey drift ratio,  $IDR$ . The performance assessment is further discussed in the next sections for tsunamis oriented in  $x$  and  $y$  directions, respectively.

It should be noted that both flexural and shear capacity of RC columns are affected by the reduction of axial load in columns due to the uplift pressure induced by buoyancy [25]. The effect of uplift pressure on the axial load,  $P$ , in ground storey columns during the VDPO-BI is shown in Fig. 10a and b for the two configurations T\_X1 and T\_X4, respectively. In configuration T\_X1 (i.e., bare frame), exterior infill walls and partitions are not considered in the dead loads (Fig. 10a). Conversely, in configuration T\_X4 the actual distribution of infill walls and partitions, as shown in Fig. 4a, is taken into account in the finite element model during the application of gravity loads. This leads to a non-uniform distribution of axial loads in ground storey columns that affect the overall performance assessment (Fig. 10b). The axial load histories show a strong reduction of compression loads on columns during the incremental analysis when the inundation depth reaches the bottom of first storey beams (i.e., 2.5 m for the case-study). Hence, neglecting tsunami-induced vertical loads during the structural assessment can lead to a dangerous overestimation of the actual capacity of existing buildings.

### 5.2.1. Tsunami in the $x$ direction

The performance levels achieved for each investigated configuration are analysed in Fig. 11, which shows the structural elements in which each performance level is first achieved and the corresponding inundation depth. This helps illustrate the effect of the exterior infill walls, in both their in-plane and out-of-plane directions, on the structural damage

distribution and evolution. It should be noted that for the performance level F2, the two hinges can either develop at the top and bottom of the columns or at the top/bottom and midspan of the columns, due to the in-plane effect of exterior half walls (i.e., T\_X3, T\_X4 and SSE\_X2).

Configuration T\_X1 (i.e., bare frame) develops a soft storey failure mechanism with the development of plastic hinges at the top and bottom of all ground storey columns, at an inundation depth of 4.6 m (Fig. 11b). This mechanism is to be expected, due to the structural typology being very close to a shear-type frame and lateral loads that are very large at the bottom of the structure. However, all ground storey columns are observed to achieve a local shear failure at an inundation depth of 4.4 m (Fig. 11c), preceding the performance level F2. Hence, a global shear failure dominates the collapse response of the structure.

Configuration T\_X2 experiences an eccentric behaviour due to the load asymmetry caused by the residual parts of masonry connected to the frame. This induces biaxial bending in columns reducing both flexural and deformation capacity [46]. For this reason, a different distribution and evolution of performance levels is observed in comparison with T\_X1. The performance level F2 is achieved at an inundation depth of 3.6 m (28% less than T\_X1). The shear failure is achieved first for an inundation depth of 2.6 m on columns with attached remaining parts of infill walls, since these members have a greater impacting surface and hence subjected to higher lateral loads than others.

In configuration T\_X3, the half wall masonry struts increase the lateral stiffness and the flexural capacity of the building (Fig. 9a), allowing for the achievement of performance level F2 for an inundation depth of 4.1 m (14% increase with respect to configuration T\_X2). The infill struts also modify the achievement of performance level S ( $H_w = 2.8$  m), since they contribute in redistributing the shear forces and reducing the shear acting on back frame columns (11 to 19). This results in a reduction of elements experiencing a shear failure with respect to configuration T\_X2.

The overall flexural performance of configuration T\_X4 (Fig. 9a) is close to the one of configuration T\_X3 for the case-study. Indeed, no significant differences are observed in the achievement of performance levels F1 and F2 for the two configurations (Fig. 11a and b). However, the explicit consideration of the time at failure of exterior walls (that is reached for  $H_w = 1.5$  m when  $Fr = 1$ ) reveals the very premature shear failure of seaward columns (1 and 11) in configuration T\_X4 for an inundation depth of 1.2 m - see Fig. 11c. Indeed, before the OOP collapse of exterior infill walls, only the seaward columns carry the tsunami lateral pressure calculated over the entire length of the infill. This leads to high shear forces acting on seaward columns that cannot be captured with a simplified model as in configuration T\_X3, which merely depicts

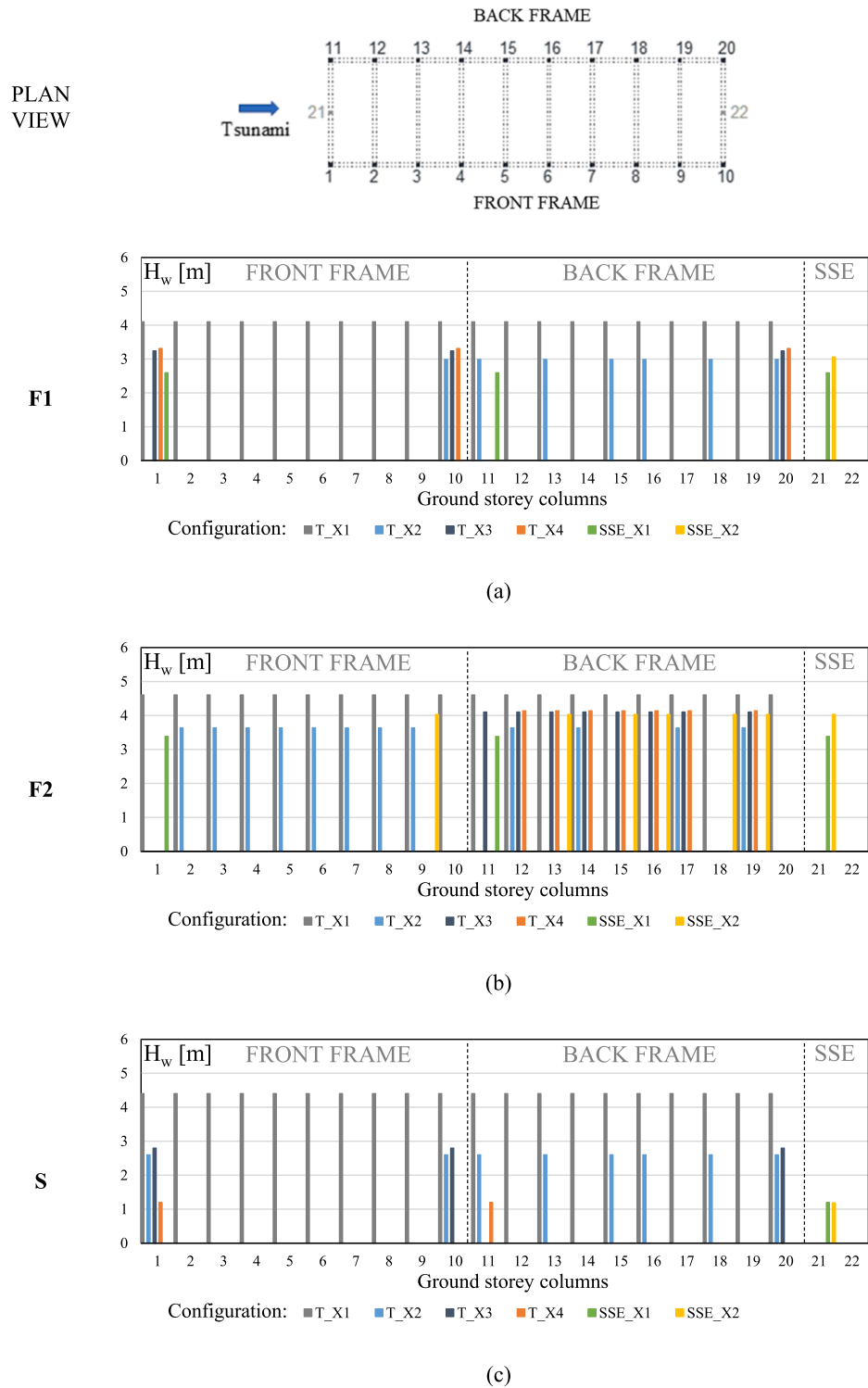


Fig. 11. Performance levels for tsunami oriented in x direction: F1 (a), F2 (b) and S (c).

exterior walls as having been blown out (right at the outset).

The non-breakaway infill walls negatively affect the performance of the SSE design. Indeed, the configuration SSE\_X1 achieves the performance level F2 for an inundation depth of 3.4 m (19% less than configuration T\_X4). This is because all drag forces are concentrated on the three seaward columns only (columns 1, 11 and 21). However, assuming typical breakaway infill walls for the SSE design (SSE\_X2) leads to an improvement in the flexural performance of the building, achieving the performance level F2 for an inundation depth of 4.0 m

(20% more than SSE\_X1 and only 3% less than T\_X4). The shear failure is not much affected by the SSE design; indeed, performance level S is achieved at the same inundation depth for configurations SSE\_X1, SSE\_X2 and T\_X4, and happens before the OOP failure of exterior infill walls.

The performance assessment shows that corner columns and rear frame columns are more prone to develop flexural damage for tsunamis in the x direction (Fig. 11b). Furthermore, it is evident that the shear failure of columns is a major problem for all the configurations



Fig. 12. Shear failure observed in a corner column of a typical school building after the 2004 tsunami.

investigated. This observation is consistent with previous numerical studies [4,7] and with observations of damage on the typical schools under investigation after the 2004 tsunami - see Fig. 12 (which corresponds to column 1 or 10 in Fig. 11c).

### 5.2.2. Tsunami in the $y$ direction

The performance levels achieved for each investigated configuration under tsunami loading in the  $y$  direction are shown in Fig. 13. Observations previously made for tsunamis in  $x$  direction also apply for tsunamis acting along the  $y$  direction of the school building.

For the typical school configuration, it is clear that neglecting the remaining parts of masonry infill walls attached to the back frame columns leads to an overestimation of the actual capacity of the structure. Indeed, performance level F2 is achieved at inundation depths of 4.7 m and 3.8 m (Fig. 13b), respectively for T\_Y1 and T\_Y2 (20% of difference). Furthermore, it is seen to lead to an overestimation of performance level S, ignoring the possible premature shear failure of back frame columns (Fig. 13c).

The in-plane capacity of the full walls in configuration T\_Y3 significantly increases the lateral capacity and stiffness of the building, allowing it to achieve performance level F2 for an inundation depth of 4.8 m (20% greater than T\_Y2).

The SSE design with non-breakaway infill walls (SSE\_Y1) has a reduced capacity at performance level F2 with respect to the previous configurations, achieving an inundation depth of 3.3 m. Conversely, configuration SSE\_Y2 reaches performance level F2 for an inundation depth of 4.1 m, that is 22% greater than SSE\_Y1 but 15% lower than the typical configuration T\_Y3. In terms of performance level S, the shear failure of back frame columns is detected at almost the same inundation depth for all configurations except for the bare one (T\_Y1).

### 5.3. Sensitivity of structural performance to the Froude number

The sensitivity of the structural performance levels to the tsunami Froude number ( $Fr$ ) assumed is now analysed. The VDPO-BI analysis is performed for  $Fr$  numbers varying between 0.4 and 2.0, in order to be representative of a wide range of flow regime conditions. In fact, Froude numbers for historical tsunamis have typically been less than 2.0 [47].

The effect of the  $Fr$  number is first shown on the typical school building in configuration T\_X4, to point out the sensitivity of the performance of structural and non-structural members (i.e., exterior infill walls) to this parameter. The envelope curves for performance levels F2 and S, expressed by means of the inundation depth as a function of the imposed  $Fr$  number, are shown in Fig. 14. The Figure also presents the envelope curves for the OOP failure of exterior infill walls at ground and first storeys as a function of the  $Fr$  number.

The plots show that shear failure always occurs before the OOP failure of exterior infill walls, which is strongly affected by the  $Fr$

number. Indeed, for increasing  $Fr$  number (i.e., increasing drag force), the inundation depth corresponding to the OOP failure of the infill walls is non-linearly reduced. The performance level F2 of the structure is similarly affected by the  $Fr$  number. Hence, the uncertainties in the hazard estimate (i.e., maximum inundation depth and velocity or  $Fr$  number) can strongly affect the capacity assessment of a structure. For the case study of T\_X4, performance level 2 is achieved for an inundation depth of 5.3 m if  $Fr = 0.6$  and of 3.0 m if  $Fr = 2.0$  (43% reduction).

A sensitivity analysis is then performed to investigate the structural capacity of typical (T\_X4 and T\_Y3) and SSE design (SSE\_X1, SSE\_X2 and SSE\_Y1, SSE\_Y2) under different  $Fr$  numbers. The relevant envelope curves are reported in Fig. 15a and b for tsunami oriented in the  $x$  and  $y$  directions, respectively. Only performance level F2 is considered for the sensitivity analysis, since performance level S has been shown as not sensitive to the typical or SSE school design configurations. Hence, the trend of performance level S derived for T\_X4 in Fig. 14 can be considered representative for both configurations.

The sensitivity of performance level F2 to the tsunami drag properties is clearly visible for all the investigated configurations in Fig. 15, with  $H_w$  values at  $Fr = 0.6$  virtually halved at one of 2.0. Furthermore, in terms of tsunami inundation depth, the typical configuration (T\_X4 and T\_Y3) shows a better performance with respect to the two SSE design configurations herein investigated, independent of the flow  $Fr$  number. Only for tsunamis in the  $x$  direction and  $Fr$  number ranging between 1 and 1.2, are similar capacities achieved for configurations T\_X4 and SSE\_X2. It is also shown that the SSE design with traditional breakaway infill walls performs better than the one with non-breakaway infill walls for the range of  $Fr$  numbers investigated.

## 6. Summary and conclusions

This paper presents a study on the effect of exterior masonry infill walls in both their in-plane and out-of-plane directions for the assessment of the structural performance of RC frame buildings subjected to tsunami-induced loads. The methodology to assess the behaviour of RC frames with breakaway infill walls, termed VDPO-BI, is first illustrated. Then it is applied to Sri Lankan school buildings to show the role of infill walls on the performance of the building. Different model configurations, based on assumptions made on the damage experienced by the exterior infill walls, are analysed. Furthermore, a new design configuration proposed by the Sri Lankan Society of Structural Engineers (SSE) after the 2004 tsunami for improving school redundancy against scour problems is also investigated, and the performance compared with the typical school design ones. Finally, the sensitivity of the structural performance to the hydrodynamic properties of the tsunami flow, expressed by means of the Froude number, is explored for both typical and SSE design configurations.

The results show that the uncertainties arising with the in-plane and out-of-plane behaviour and failure of exterior infill walls under tsunami-induced loads can strongly affect the performance and damage assessment of a frame structure. Based on the analysis results, the following general conclusions can be drawn:

- The in-plane behaviour of exterior infill walls increases the flexural capacity and lateral stiffness of the structure. For the case study, it improved the flexural response of the structure, with performance level F2 (defined as the first development of two hinges in a column) being achieved at tsunami inundation depths that were 14%-20% larger than for the model where this contribution is neglected;
- Assuming that exterior infill walls collapse at the start of the structural analysis but including the portions of masonry that can be still attached to the frame may represent a simplified but acceptable solution for providing realistic estimates of the flexural performance of a structure. This would only be appropriate for infill walls with low out of plane resistance. This assumption will, however, lead to an

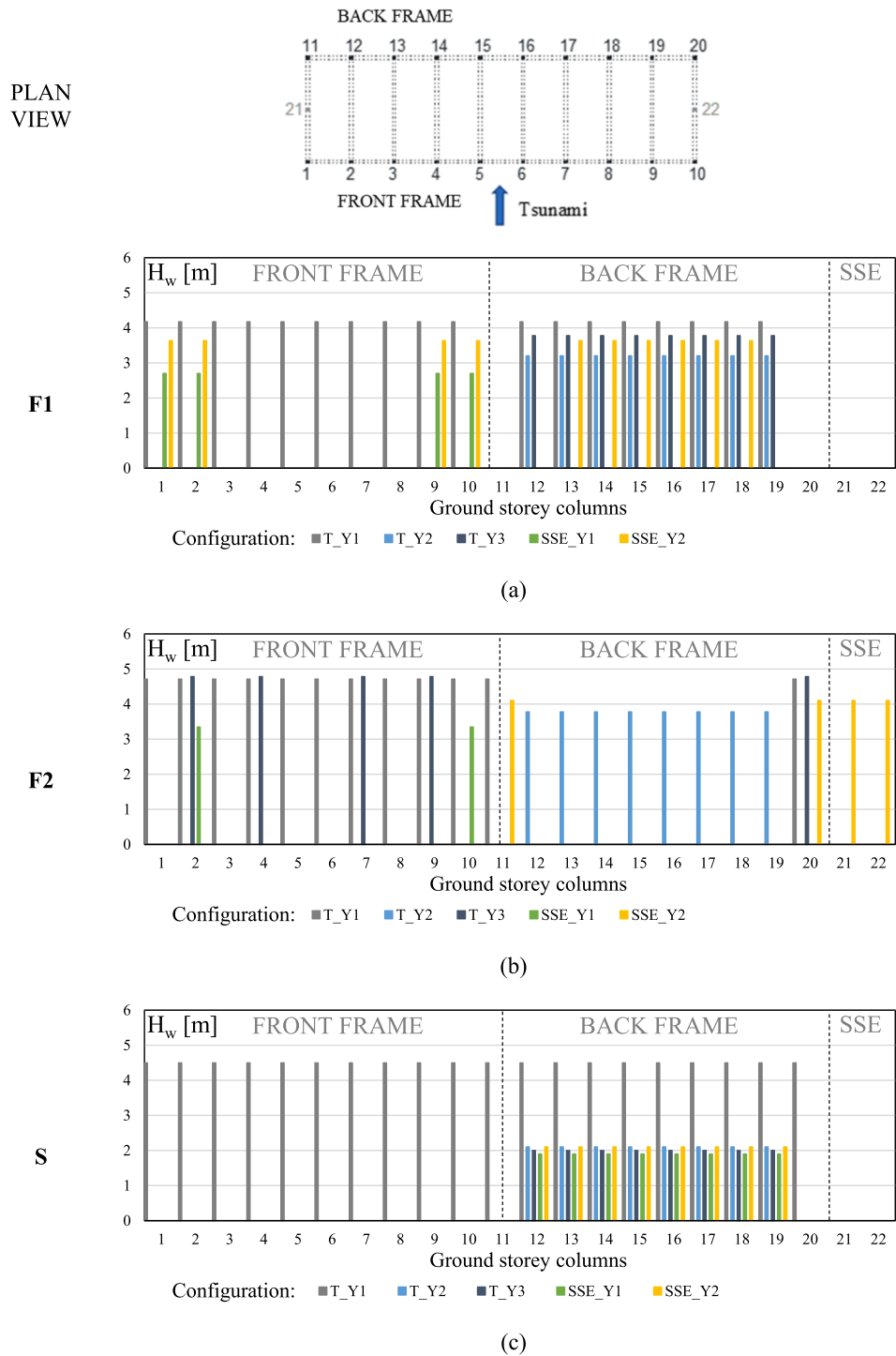


Fig. 13. Performance levels for tsunami oriented in y direction: F1 (a), F2 (b) and S (c).

overestimation of the performance level associated with the shear failure of columns;

- A good estimate of the location and occurrence of shear failure in structural elements can only be achieved by explicitly considering the OOP behaviour and failure of exterior infill walls during an incremental tsunami load analysis;
- The Froude number strongly affects the performance of both structural and non-structural components. A non-linear decreasing trend of performance levels is observed for increasing Froude numbers. Hence, it is important that realistic estimates of the tsunami

characteristics be obtained and used in the analysis in order to perform a reliable capacity assessment;

- The use of non-breakaway infill walls is seen to consistently result in premature structural failure mechanisms (for the structures investigated), associated with the concentration of drag forces on seaward columns only;
- The shear failure of ground storey columns is the first performance level achieved for all the configurations investigated, confirming that this failure mechanism is a major problem in the case of tsunami loading if a perfect connection between masonry and columns is assumed.

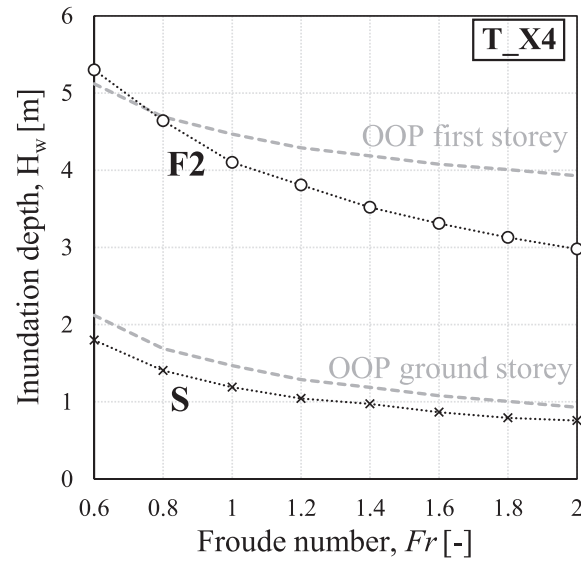


Fig. 14. Sensitivity of performance levels F2 and S to the  $Fr$  number for configuration T\_X4.

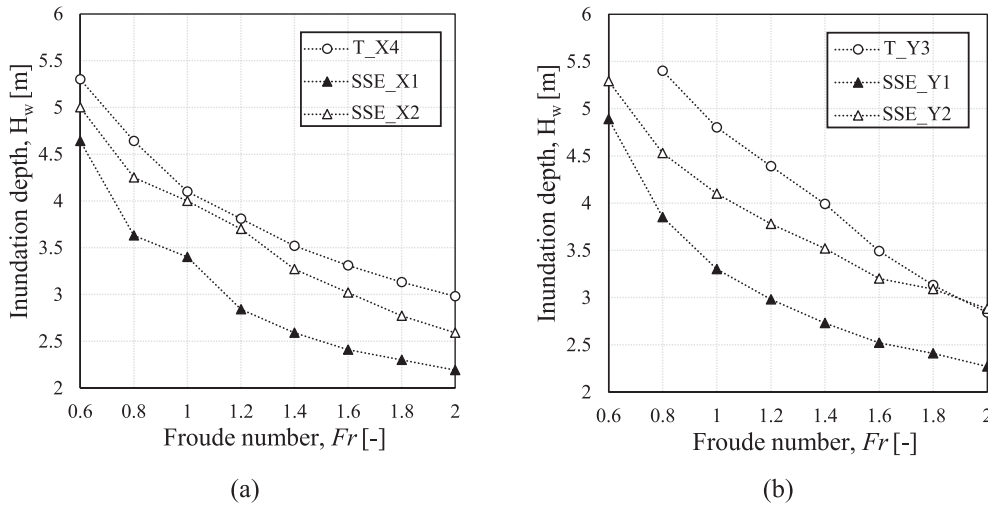


Fig. 15. Sensitivity of performance level F2 to the  $Fr$  number for tsunami oriented in the x (a) and y (b) directions.

Irrespective of the tsunami flow  $Fr$  number, the SSE design for new school buildings, albeit proposed for increasing resilience against scour, does not provide a significant improvement in the lateral capacity of the structure under tsunami loading. This is mainly due to the adoption of non-breakaway infill walls. Hence, based on this study, to reduce the drag forces acting on columns during the tsunami inundation, the adoption of masonry walls with low OOP capacity and/or the isolation of infill panels from the surrounding columns may represent sound solutions to improve the overall performance of Sri Lankan school buildings, and RC frame structures more generally. However, the loss of content deriving from the flooding of ground storey levels after the OOP failure of exterior infill walls needs also to be accounted for, and for some critical infrastructures (i.e., hospitals) cannot be accepted. From a multi-hazard perspective, considering earthquake and tsunami in sequence, the OOP performance of infill walls may also represent a critical issue. Indeed, the OOP failure of infill walls is an undesired damage mechanism for seismic design, and OOP strengthening is a common seismic retrofit solution for such non-structural components. This would increase tsunami forces on the structure. Conversely, damage to infill walls due to seismic actions can reduce their OOP resistance

under subsequent tsunami loading. Hence, integrated design and retrofit approaches that include the considerations herein identified for tsunami loading should be developed for structures exposed to multiple hazards.

The study provides useful results for the capacity assessment of structures in probabilistic frameworks, highlighting the main sources of uncertainty in the modelling of RC structures with breakaway infill walls and their role on the performance of structural and non-structural members. The VDPO-BI methodology herein adopted to assess the performance of the school buildings under tsunami loading appears to be a very appropriate solution for the development of analytical tsunami fragility functions, accounting for the uncertainties related to the behaviour and failure of exterior infill walls in both their in-plane and out-of-plane directions. Further developments of the VDPO-BI methodology will look at a generalized inclusion of tsunami-induced uplift loads (including buoyancy due to enclosed space) within the non-linear static analysis framework. Future works will also explore the definition of a probabilistic framework to assess the vulnerability of existing Sri Lankan school buildings under different tsunami inundation scenarios.

## Declaration of Competing Interest

The authors declare that they have no known competing financial interests or personal relationships that could have appeared to influence the work reported in this paper.

## Acknowledgements

The research for this paper is funded by the UK Global Challenges Research Fund project ReSCOOL (Resilience Of Schools To Extreme Coastal FLOODing Loads), awarded to Professor Tiziana Rossetto by Research England (Award 177813).

## Appendix A. Supplementary material

Supplementary data to this article can be found online at <https://doi.org/10.1016/j.engstruct.2021.111920>.

## References

- [1] D'Ayala D, Galasso C, Nassirpour A, Adhikari RK, Yamin L, Fernandez R, et al. Resilient communities through safer schools. *Int J Disaster Risk Reduct* 2020;45: 101446.
- [2] ASCE (2017), Minimum Design Loads and Associated Criteria for Buildings and Other Structures. ASCE/SEI 7-16. Reston, VA, USA.
- [3] Del Zoppo M, Rossetto T, Di Ludovico M, Protà A. Assessing the effect of tsunami-induced vertical loads on RC frames. In: Proceedings of 1st fib Italy YMG symposium on concrete and concrete structures; 2019. p. 206–12.
- [4] Del Zoppo M, Di Ludovico M, Protà A. Methodology for Assessing the Performance of RC Structures with Breakaway Infill Walls under Tsunami Inundation. *ASCE J Struct Eng* 2021;147(2):0002900.
- [6] Foytong P, Ruangrassamee A, Lukkunaprasit P. Correlation analysis of reinforced concrete building under tsunami loading pattern and effect of masonry infill walls on tsunami load resistance. *IES J Part A Civ Struct Eng* 2013. <https://doi.org/10.1080/19373260.2012.756125>.
- [7] Petrone C, Rossetto T, Goda K. Fragility assessment of a RC structure under tsunami actions via nonlinear static and dynamic analyses. *Eng Struct* 2017;136:36–53.
- [8] Alam MS, Barbosa AR, Scott MH, Cox DT, van de Lindt JW. Development of physics-based tsunami fragility functions considering structural member failures. *J Struct Eng* 2017;44(3):04017221.
- [9] Macabuag J, Rossetto T, Lloyd T. Structural analysis for the generation of analytical tsunami fragility functions. In: 10th International conference on urban earthquake engineering; 2014.
- [10] Attary N, van de Lindt JW, Unnikrishnan VU, Barbosa AR, Cox DT. Methodology for development of physics-based tsunami fragilities. *J Struct Eng* 2017;143(5).
- [11] Rossetto T, De la Barra C, Petrone C, De la Llera JC, Vásquez J, Baiguera M. Comparative assessment of nonlinear static and dynamic methods for analysing building response under sequential earthquake and tsunami. *Earthquake Eng Struct Dyn* 2019;48(8):867–87.
- [12] Petrone C, Rossetto T, Baiguera M, De la Barra Bustamante C, Ioannou I. Fragility functions for a reinforced concrete structure subjected to earthquake and tsunami in sequence. *Eng Struct* 2020; 205, 110120.
- [13] Karafagka S, Fotopoulou S, Pitolakis K. Analytical tsunami fragility curves for seaport RC buildings and steel light frame warehouses. *Soil Dyn Earthquake Eng* 2018;112:118–37.
- [14] Medina S, Lizarazo-Marriaga J, Estrada M, Koshimura S, Mas E, Adriano B. Tsunami analytical fragility curves for the Colombian Pacific coast: a reinforced concrete building example. *Eng Struct* 2019;196:109309.
- [15] Nanayakkara KIU, Dias WPS. Fragility curves for structures under tsunami loading. *Nat Hazards* 2016;80:471–86. <https://doi.org/10.1007/s11069-015-1978-1>.
- [16] Donga, Mario, Patrizia Bitter. Teaching Disaster Risk Management in Sri Lanka's Schools. Experience Since the 2004 Tsunami. GTZ, Eschborn; 2008.
- [17] Guidelines for buildings at risk from natural disasters. Society of Structural Engineers, Sri Lanka., Colombo, October 2005, 22 pp.
- [18] Foster ASJ, Rossetto T, Allsop W. An experimentally validated approach for evaluating tsunami inundation forces on rectangular buildings. *Coast Eng* 2017; 128:44–57.
- [19] McGovern DJ, Chandler I, Allsop W, Robinson T, Rossetto T. Pneumatic long-wave simulation of tsunami-length waveforms and their runup. *Coast Eng* 2017:1–23.
- [20] Yeh H, Barbosa AR, Ko H, Cawley JG. Tsunami loadings on structures: Review and analysis. *Coast Eng Proc* 2014;1(34):4.
- [21] Cavaleri L, Ciraolo G, Ferrotto MF, La Loggia G, Lo Re C, Manno G. Masonry structures subjected to tsunami loads: Modeling issues and application to a case study. *Structures* 2020;27:2192–207.
- [22] Robertson IN. Tsunami Loads and Effects: Guide to the Tsunami Design Provisions of ASCE 7–16. ASCE Publications; 2020.
- [23] Baiguera M, Rossetto T, Robertson IN, Petrone C. Towards a tsunami nonlinear static analysis procedure for the ASCE 7 standard. In: ICONHIC 2019 2nd International Conference on Natural Hazards & Infrastructure, Chania, Greece; 2019.
- [24] Comité Européen de Normalisation. Eurocode 6, Design of masonry structures. EN 1996-1-1, Part 1-1: General rules for reinforced and unreinforced masonry structures, CEN, Brussels; 2005.
- [25] Qi ZX, Eames I, Johnson ER. Force acting on a square cylinder fixed in a free-surface channel flow. *J Fluid Mech* 2014;756:716–27.
- [26] Latcharote P, Suppasri A, Yamashita A, Adriano B, Koshimura S, Kai Y, et al. Possible Failure Mechanism of Buildings Overturned during the 2011 Great East Japan Tsunami in the Town of Onagawa. *Front Built Environ* 2017;3:16. <https://doi.org/10.3389/fbuil.2017.00016>.
- [27] Del Zoppo M, Rossetto T, Di Ludovico M, Protà A, Robertson I. Structural Response Under Tsunami-induced Vertical Loads. In: Proceedings of the 17th world conference on earthquake engineering, 17WCEE, Sendai, Japan; Sept., 2020.
- [28] Dias WPS, Mallikarachchi HMYC. Tsunami – planning and design for disaster mitigation. *Struct Eng* 2006;84(6):25–9.
- [29] Dias P, Dissanayake R, Chandratilake R. Lessons learned from tsunami damage in Sri Lanka. *ICE Proc Civil Eng* 2006;159(2):74–81. <https://doi.org/10.1680/cien.2006.159.2.74>.
- [30] McKenna F, Fenves GL, Filippou FC. OpenSees. Berkeley: University of California; 2010.
- [31] Spacone E, Filippou F, Taucer F. Fiber beam-column model for non-linear analysis of R/C frames: Part I. Formulation. *Earthquake Eng Struct Dynam* 1996;25:711–25.
- [32] Spacone E, Filippou F, Taucer F. Fiber beam-column model for non-linear analysis of R/C frames: Part II. Applications. *Earthquake Eng Struct Dynam* 1996;25: 727–42.
- [33] Comité Européen de Normalisation. Eurocode 8, Design of structures for earthquake resistance — Part 3: Assessment and retrofitting of buildings. EN 1998-1, CEN, Brussels; 2005.
- [34] Furtado A, Rodrigues H, Varum H, Arêde A. Mainshock-aftershock damage assessment of infilled RC structures. *Eng Struct* 2018;175:645–60.
- [35] Ricci P, Di Domenico M, Verderame GM. Empirical-based out-of-plane URM infill wall model accounting for the interaction with in-plane demand. *Earthquake Eng Struct Dyn* 2018;47(3):802–27.
- [36] Panagiotakos TB, Fardis MN. Seismic response of infilled RC frames structures. In: 11th world conference on earthquake engineering (No. 225); 1996.
- [37] Crisafulli FJ. Seismic behaviour of reinforced concrete, structures with masonry infill walls. PhD Dissertation. University of Canterbury; 1997.
- [38] FEMA 365. Pre-standard and Commentary for the Seismic Rehabilitation of Buildings, Federal Emergency Management Agency, Washington, D.C., USA; 2000.
- [39] Thamboo JA. Material characterisation of thin layer mortared clay masonry. *Constr Build Mater* 2020;230:116932.
- [40] Popovics S. A numerical approach to the complete stress strain curve for concrete. *Cem Concr Res* 1973;3(5):583–99.
- [41] Jirsa J, Karsan I. Behavior of concrete under compressive loadings. *J Struct Divis* 1969;95(12):2543–63.
- [42] Filippou FC, Popov EP, Bertero VV. Effects of bond deterioration on hysteretic behavior of reinforced concrete joints. Report EERC 83-19, Earthquake Engineering Research Center, University of California, Berkeley; 1983.
- [43] Hemant BK, Durgesh CR, Sudhir KJ. Stress-Strain Characteristics of Clay Brick Masonry under Uniaxial Compression. *J Mater Civil Eng (ASCE)* 2007;19(9): 728–39.
- [44] Konthesingha K, Jayasinghe C, Nanayakkara S. Bond and Compressive Strength of Masonry for Locally Available Bricks. *Inst Eng Sri Lanka* 2007;2(4):7–13.
- [45] Ruangrassamee A, Yanagisawa H, Foytong P, Lukkunaprasit P, Koshimura S, Imamura F. Investigation of Tsunami-Induced Damage and Fragility of Buildings in Thailand after the December 2004 Indian Ocean Tsunami. *Earthquake Spectra* 2006;22(3):377–401.
- [46] Del Zoppo M, Di Ludovico M, Verderame GM, Protà A. Experimental behavior of nonconforming RC columns with deformed bars under constant axial load and fixed biaxial bending. *J Struct Eng* 2017;143(11):04017153.
- [47] Matsutomi H, Okamoto K. Inundation flow velocity of tsunami on land. *Isl Arc* 2010;19(3):443–57.